Research on Engineering Structures & Materials
www.jresm.org
Research Group

Research Article

Predictive modeling of glass powder and activator effects on slag-based geopolymers via central composite design

Amirouche Berkouche[1,a], Ahmed Abderraouf Belkadi[*,1,b], Salima Aggoun[2,c], Redha Hammouche[3,d], Samir Benaniba[4,e]

[1]*Dept. of Civil Eng., Mohamed El-Bachir El-Ibrahimi University of Bordj Bou Arreridj, El-Anasser, Algeria*
[2]*CY Cergy Paris Université, L2MGC, F-95000 Cergy, France*
[3]*Materials and Durability of Construction Laboratory, Dept. of Civil Eng., Faculty of Science and Technology, Frère Mentouri University of Constantine 1, Constantine 25000, Algeria*
[4]*Mechanical Eng. Dept., Faculty of Sciences and Technology, University Mohamed El Bachir El Ibrahimi of Bordj Bou Arreridj, El-Anasser, Algeria*

Article Info

Article history:

Received 03 July 2024
Accepted 13 Sep 2024

Keywords:

Geopolymer;
Modeling;
Glass powder;
Optimization;
Central composite design

Abstract

This study investigates the effects of glass powder (GP) content and activator-to-precursor (Ac/Pr) ratio on the properties of slag-based geopolymer mortars using a central composite design approach. GP content ranging from 0% to 30% and Ac/Pr ratios between 0.65 and 0.75 were examined. Response surface methodology was utilized to construct predictive models for slump, 28-day compressive strength, and porosity. Scanning electron microscopy and energy dispersive X-ray spectroscopy were utilized to analyze the microstructure and chemical composition of the geopolymer matrices. Results indicate that both GP content and Ac/Pr ratio significantly influence mortar properties. Increasing GP content and Ac/Pr ratio generally improved workability, while optimal mechanical performance was achieved at moderate levels of both factors. The optimal formulation, determined through desirability analysis, consisted of 18.2% GP content and 0.72 Ac/Pr ratio, yielding predicted outcomes of 16.53 cm slump, 46.64 MPa compressive strength, and 15.85% porosity. This study demonstrates the potential of incorporating waste glass in slag-based geopolymers and provides a framework for optimizing mix designs to achieve desired performance characteristics.

1. Introduction

The global construction industry faces an unprecedented challenge in the 21st century: meeting the growing demand for infrastructure while simultaneously reducing its environmental impact. At the heart of this challenge lies the production of cement, a process responsible for approximately 8% of worldwide CO_2 emissions [1]. This staggering figure underscores the urgent need for sustainable alternatives that can mitigate the environmental footprint of construction activities without compromising on performance or durability. In recent decades, geopolymers have emerged as a promising solution to this pressing issue, offering comparable or superior performance to conventional cement while significantly reducing associated carbon emissions [2, 3].

Geopolymers, a term coined by Joseph Davidovits in the 1970s [4], represent a class of inorganic polymers synthesized through the alkaline activation of aluminosilicate materials, including metakaolin, fly ash, and ground granulated blast furnace slag (GGBFS).

*Corresponding author: ahmedabderraouf.belkadi@univ-bba.dz
[a] orcid.org/0009-0004-1540-139X; [b] orcid.org/0009-0002-5978-9774; [c] orcid.org/0000-0002-2757-1263; [d] orcid.org/0009-0004-4458-8309
DOI: http://dx.doi.org/10.17515/resm2024.337st0703rs

These materials are rich in silicon (Si) and aluminum (Al), which are essential for the geopolymerization process [5, 6]. The geopolymerization process begins with the dissolution of these precursor materials in a highly alkaline environment, typically provided by a combination of sodium or potassium hydroxide and silicate solutions [7]. Once dissolved, the aluminate and silicate species undergo condensation reactions, forming a gel-like network of aluminosilicate hydrates [8]. This network further polymerizes into a three-dimensional matrix, primarily consisting of sodium-aluminosilicate-hydrate (N-A-S-H) gels in low calcium systems or calcium-aluminosilicate-hydrate (C-A-S-H) gels in high calcium systems like those containing GGBFS [9, 10]. This process is responsible for the development of mechanical strength and durability in geopolymer materials [11], making them suitable for various construction applications.

These innovative binding agents offer numerous advantages over traditional Portland cement, including drastically reduced CO_2 emissions—up to 80% less compared to conventional cement production [3]. To regulate sustainability, one must control the kind and quantity of binder used in concrete mixtures, since they account for over 90% of the CO_2 in the mixture [12]. While regular Portland cement emits 306 kg CO_2/m^3 for the same mechanical qualities, geopolymer releases just 169 kg CO_2/m^3, a 45% reduction in emissions, as stated by Biernacki et al. [12]. Additionally, according to Davidovits [13], fly ash-based geopolymers can achieve CO_2 emissions in the range of 0.09 to 0.25 kg CO_2 per kilogram, which translates to a 75 to 90% reduction compared to conventional cement.

Moreover, geopolymers enable the utilization of various industrial by-products, contributing to circular economy principles and waste reduction. Many geopolymer formulations exhibit enhanced durability, demonstrating superior resistance to chemical attack, fire, and extreme temperatures [14], [15], [16]. Perhaps most importantly, geopolymers can achieve strength and performance characteristics that match or exceed those of traditional cement-based materials, making them a viable alternative for a wide range of construction applications.

Despite these compelling advantages, the widespread adoption of geopolymers faces several challenges related to raw material availability, mix design optimization, and long-term performance under various environmental conditions. Ongoing research efforts are focused on addressing these challenges and expanding the application of geopolymers in construction. A critical aspect of this research involves the careful selection and optimization of precursor materials, which play a crucial role in determining the properties and performance of geopolymer systems. Among the various precursors used in geopolymer production, GGBFS has gained significant attention due to its widespread availability and favorable chemical composition. GGBFS, a by-product of the iron and steel industry, is formed when molten iron blast furnace slag is rapidly cooled by water. Its chemical composition typically consists of CaO, SiO_2, and Al_2O_3 [17]. The high calcium content in GGBFS contributes to the formation of calcium silicate hydrate (C-S-H) gels in addition to the geopolymeric network [18], [19], [20], resulting in enhanced mechanical properties and reduced setting times compared to low-calcium precursors.

The Ca/Si and Si/Al ratios in geopolymer systems are critical factors that influence the reaction mechanisms, microstructure development, and ultimately, the properties of the hardened material. A higher Ca/Si ratio promotes the formation of C-S-H gels, which can coexist with the geopolymeric network [21], leading to improved mechanical properties. However, excessive calcium content can hinder the geopolymerization process by competing for available silica, potentially reducing long-term strength development [22], [23]. Similarly, the Si/Al ratio affects the degree of polymerization and the structure of the aluminosilicate network [24]. Higher Si/Al ratios generally result in increased compressive strength and improved durability due to the formation of more stable Si-O-Si

bonds [25], [26]. However, very high Si/Al ratios can lead to unreacted silica and reduced strength [27]. Optimizing these ratios is crucial for achieving the desired balance between early strength development, long-term performance, and durability of geopolymer materials.

In the quest for further enhancing the sustainability and performance of geopolymer systems, researchers have begun exploring the potential of glass powder (GP) as a supplementary precursor. Derived from recycled waste glass, GP offers a promising avenue for incorporating high-silica content materials into geopolymer mixtures. The chemical composition of GP typically includes SiO_2 [28]. This high silica content, combined with the amorphous nature of glass, makes GP an attractive material for geopolymer production, offering several potential benefits. The incorporation of GP in geopolymer systems can enhance silicon availability due to the easier dissolution of amorphous glass in alkaline media, providing readily available silica for geopolymerization reactions. The spherical shape of glass particles can contribute to better flowability of fresh geopolymer mixtures, potentially improving workability [29], [30]. Furthermore, the utilization of waste glass in geopolymers addresses the challenge of glass disposal while reducing the demand for virgin raw materials, further enhancing the environmental credentials of these alternative binding materials.

Several studies have explored the incorporation of GP in alkali-activated systems, demonstrating its potential as a supplementary precursor. Researchers have reported improved compressive strength and reduced porosity with GP addition up to 30% replacement in alkali-activated slag mortars [28], [29], [31], [32], [33]. Synergistic effects have been observed when combining GP with fly ash in geopolymer systems, leading to enhanced mechanical properties and microstructure development [34], [35]. The influence of GP fineness on the properties of alkali-activated slag concrete has also been examined, with finer GP particles leading to improved strength and durability characteristics [36], [37]. Moreover, the use of GP in combination with calcined clay for geopolymer production has shown promise, with studies reporting increased compressive strength and reduced water absorption upon GP incorporation. The introduction of GP as a silica-rich source in geopolymer systems offers several advantages for optimizing the critical Ca/Si and Si/Al ratios. The high silica content of GP allows for fine-tuning of the Si/Al ratio, potentially leading to improved mechanical properties and durability. In slag-based systems, GP can help moderate the high calcium content, promoting a more balanced formation of C-S-H gels and geopolymeric networks. The amorphous nature of GP can contribute to increased dissolution rates and overall system reactivity, potentially accelerating strength development. Furthermore, the incorporation of GP may lead to a more compact and refined microstructure [38], [39], reducing porosity and enhancing long-term performance.

Despite the promising results reported in literature, there remains a need for a comprehensive understanding of the effects of GP incorporation on the properties of slag-based geopolymer systems. Moreover, the development of predictive models for optimizing mix designs is crucial for the practical implementation of GP in geopolymer production. This research aims to address these knowledge gaps by investigating the influence of GP as a partial replacement for GGBFS on the mechanical and physical properties of eco-geopolymer mortars. The primary objective of this study is to elucidate the effects of GP replacement levels (0-30%) and activator-to-precursor ratio (Ac/Pr) on the fresh and hardened properties of slag-based geopolymer mortars. To achieve this, the response surface methodology will be utilized to develop predictive models for slump, compressive strength, and porosity as a function of GP content and Ac/Pr ratio. This approach will enable the optimization of mix designs based on desired performance criteria. Furthermore, microstructural analysis using Scanning Electron Microscopy (SEM)

coupled with Energy Dispersive X-ray (EDX) spectroscopy will be employed to examine the morphological characteristics and chemical composition of the geopolymer matrices, providing insights into the formation of C-A-S-H gels and their distribution within the microstructure. This comprehensive analysis will elucidate the relationship between mix composition, microstructural development, and macroscopic properties of the geopolymer mortars

By addressing these research goals, this study aims to contribute to the development of more sustainable and high-performance geopolymer materials, paving the way for their increased adoption in construction applications. The findings of this research will provide valuable insights into the optimal utilization of GP in slag-based geopolymer systems, offering a pathway for the valorization of waste glass while enhancing the environmental credentials of alternative cementitious materials. Ultimately, this work seeks to advance the state-of-the-art in eco-friendly construction materials, contributing to the global effort to reduce the environmental impact of the built environment while meeting the growing demands for infrastructure development.

2. Materials and Methods

2.1. Materials

This study utilized several key materials to produce the slag-based geopolymer mortars, such as GBFS, GP, sand, and alkaline activators. GGBFS and GP served as the primary precursors for the geopolymer binder. The GGBFS was sourced from a regional steel manufacturer (El-Hadjar complex, Annaba, Algeria) as spherical grains with a particle size of 0/5 mm, which were then crushed to achieve a fineness of 237.1 m^2/kg. The glass waste (sourced from local recycling facilities in Setif, Algeria) was subjected to grinding processes, resulting in a fineness of 280.8 m^2/kg. The appearance of both GGBFS and GP is displayed in Fig. 1.

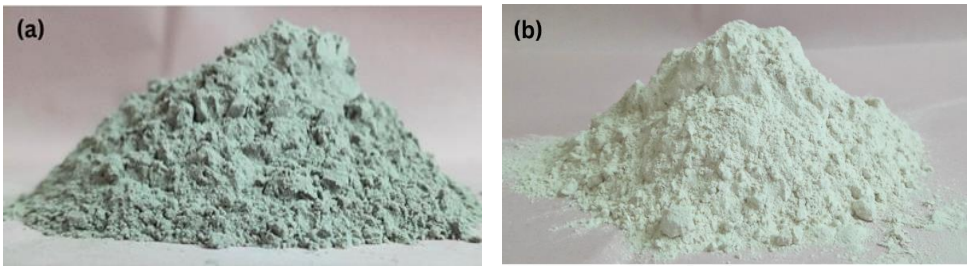

Fig. 1. Visual appearance of precursors (a) GGBFS (b) GP

The chemical compositions of GGBFS and GP are presented in Table 1, which shows their major oxide constituents. Table 2 provides the physical properties of GGBFS and GP, including their densities and Blaine surface areas, which are crucial parameters affecting their reactivity and water demand in the mixtures.

Table 1. Chemical composition of precursors

%	CaO	SiO_2	Al_2O_3	Fe_2O_3	K_2O	Na_2O	MgO	SO_3	LOI
GGBFS	43.1	41.2	6.99	2.9	0.33	0.5	4.9	0.25	0.03
GP	8.31	70.97	1.36	0.47	0.56	14.72	2.41	0.34	0.79

Table 2. Physical properties of precursors

	GGBFS	GP
Bulk density (kg/m^3)	2951	2533
Specific surface area (m^2/kg)	237.1	280.8

The particle size distribution of GGBFS and GP was determined using a laser diffraction analyzer (Cilas 1090), which provides detailed information on particle size by measuring the angle and intensity of light scattered by particles in suspension. This method allows for precise determination of particle size distribution across a wide range of sizes, ensuring the reliability of the data presented. Fig. 2 illustrates the particle size distributions of GGBFS and GP, offering insights into their fineness and potential packing behavior within the geopolymer matrix The particle size distribution of GGBFS ranges from 1.65 µm (d10) to 56.16 µm (d90), meaning that 10% of GGBFS particles are finer than 1.65 µm, and 90% are finer than 56.16 µm. This indicates a broader range of particle sizes, which can contribute to a denser microstructure due to improved packing efficiency. In contrast, the GP's particle size distribution is more uniform, ranging from 4.18 µm (d10) to 68.37 µm (d90), with a median particle size of 18.55 µm. This distribution suggests different mechanical performance characteristics, as the uniformity of GP may influence the reactivity and strength development differently from GGBFS.

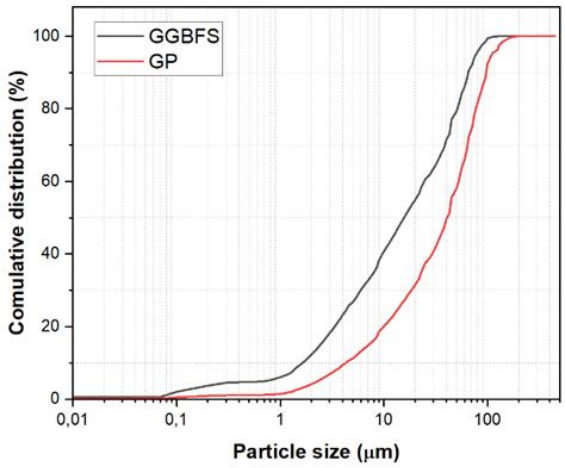

Fig. 2. Particle size distribution of precursors

The broader particle size distribution observed in GGBFS offers the potential for a denser microstructure due to better packing efficiency. When particles of varying sizes are present, smaller particles can fill the voids between larger particles, leading to a more compact arrangement and reducing the overall porosity of the material [40], [41]. This reduction in porosity is directly correlated with increased compressive strength, as the denser structure can better resist the applied loads without fracturing [42]. Additionally, a well-packed microstructure may also contribute to improved durability by reducing the permeability of the geopolymer [43]. On the other hand, the more uniform particle size distribution of GP might lead to different mechanical performance characteristics. While the uniformity in size can promote more consistent reactivity throughout the matrix, it may also result in a less dense microstructure compared to GGBFS if the packing is not optimized. This could lead to higher porosity and potentially lower compressive strength

[44]. However, the use of a uniform particle size distribution can also be advantageous in controlling the workability of the geopolymer mixture, as it may prevent excessive segregation or bleeding, ensuring a more homogenous mixture that can be easily placed and compacted.

The alkaline activation of the precursors was achieved using a combination of sodium hydroxide (NaOH) and sodium silicate (Na_2SiO_3) solutions. NaOH was provided by the SPECILAB laboratory, distributed by the company PROCHIMA SIGMA located in Tlemcen, Algeria, with a density 2130 kg/m^3 and a purity of 99%. NaOH solution was prepared at a concentration of 10M, while Na_2SiO_3 solution contained 26% SiO_2 and 8% Na_2O by mass. The chemical properties of sodium silicates are presented in Table 3.

Table 3. Characteristics of sodium silicates used

Parameter	Composition
SiO_2 (%)	26
Na_2O (%)	8
pH	13.01
Density at 20° C	1,53
Concentration (%)	45
SiO_2/Na_2O	3.25

These activators were combined in a ratio of Na_2SiO_3 to NaOH of 3:1 to provide the optimal alkalinity and silica content for geopolymerization. The sand used in this study was sourced from the Oued Souf dunes in Algeria. This sand is characterized by its high silica content and rounded, smooth-surfaced grains, making it ideal for mortar applications. Its physical properties include an apparent density of 2623 kg/m^3, a fineness modulus of 1.99, and a sand equivalent of 86.49%. The particle size distribution of the sand is well-graded, with a maximum grain size not exceeding 4.0 mm, ensuring good workability and compact packing in the mortar matrix.

2.2. Methodology

One common statistical method for designing and optimizing experiments is the central composite design, or CCD. This research used a two-pronged approach to examine the impact of GP content (0%-30%) and Ac/Pr ratio (0.65, 0.7, and 0.75) on geopolymer mortar characteristics. With its capacity to fit quadratic models and capture higher-order interactions between the components, the CCD efficiently minimizes the number of experimental runs, making it an attractive choice. As shown in Table 4, the CCD for this investigation comprised nine distinct formulations.

Slump, compressive strength, and water-accessible porosity were the intended outcomes of the nine strategic formulations' data collection efforts. The purpose of analyzing these reactions was to shed light on how the input parameters, individually and in combination, affected the physical and mechanical characteristics of the manufactured mortars.

The optimal mix design derived from the desirability analysis, prediction expressions, response surface profiler, and analysis of variance (ANOVA) results are the products of this statistical methodology. To optimize the geopolymer mortar formulation for the intended mechanical and physical properties, these outputs offer useful insights into the effects of the input parameters and how they interact with the responses.

Table 4. Experimental runs and mix composition using CCD

Mix ID	GP (%)	Ac/Pr	GGBFS (kg/m^3)	GP (Kg/m^3)	Sodium silicate (kg/m^3)	NaOH (kg/m^3)	Sand (kg/m^3)
M1	0	0.65	587,65	0,00	286,48	95,49	
M2	15	0.65	499,50	88,15	286,48	95,49	
M3	30	0.65	411,36	176,30	286,48	95,49	
M4	0	0.7	587,65	0,00	308,52	102,84	
M5	15	0.7	499,50	88,15	308,52	102,84	1250
M6	30	0.7	411,36	176,30	308,52	102,84	
M7	15	0.75	499,50	88,15	330,55	110,18	
M8	30	0.75	411,36	176,30	330,55	110,18	
M9	0	0.75	587,65	0,00	330,55	110,18	

2.3. Sample Preparation

GGBFS, GP, and sand have been carefully weighed according to the proportions specified in the previous formulations. These dry components have been thoroughly mixed to ensure their homogeneity. At the same time, an alkaline activator solution was prepared by mixing NaOH and Na_2SiO_3 solutions in a ratio of 1 to 3 to ensure uniformity and consistency in the geopolymerization reaction [45], [46]. Then the dry mixture was combined with the activator solution using a mechanical mixer for 90 seconds, thus giving rise to a homogeneous geopolymer paste. This preparation was then poured into a spreading cone to evaluate its maneuverability before being carefully poured into molds of dimensions 4x4x4 cm^3 (Fig. 3). To facilitate geopolymerization reactions, the specimens were demolded after one day and transferred to a controlled environment, kept at a temperature of 20 ± 2 °C and a relative humidity of ≥ 95%, where they remained until they reached the desired test age.

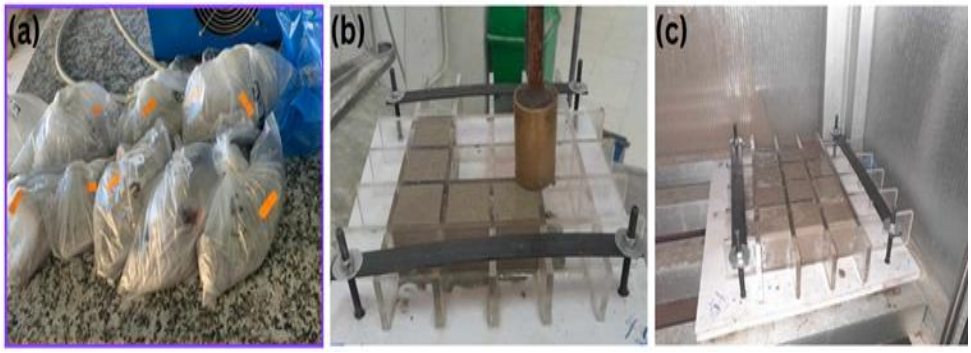

Fig. 3. Preparation of geopolymer mortars (a) preparation of raw materials (b) molding (c) curing

2.4. Experimental Tests

This study conducted three key tests to evaluate the performance of the slag-based geopolymer mortars: slump test, compressive strength test, and water accessible porosity

test. Each test was performed three times according to standard procedures to ensure reliability and reproducibility of results.

The slump test was carried out to assess the workability of the fresh geopolymer mortar mixtures (Fig. 4). The test was performed in accordance with ASTM standard [47] using a mini-slump cone. The cone, with dimensions of 70 mm top diameter, 100 mm base diameter, and 50 mm height, was filled with the fresh mortar and lifted vertically. The resulting spread of the mortar was measured in two perpendicular directions, and the average value was recorded as the slump flow.

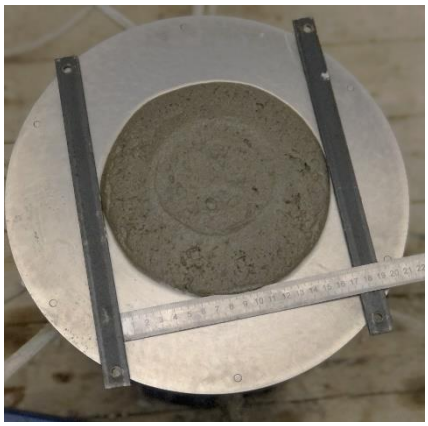

Fig. 4. Slump test of geopolymer mortar

The compressive strength of the hardened geopolymer mortars was determined following the procedures outlined in EN 196-1 standard [48] after 28 days of curing (Fig. 5). The specimens were subjected to uniaxial compression using a hydraulic testing machine. The load was applied at 5 mm/min displacement rate on a 400 kN compression capacity testing machine until failure occurred. The maximum load sustained by each specimen was recorded, and the compressive strength was calculated by dividing this load by the cross-sectional area of the specimen.

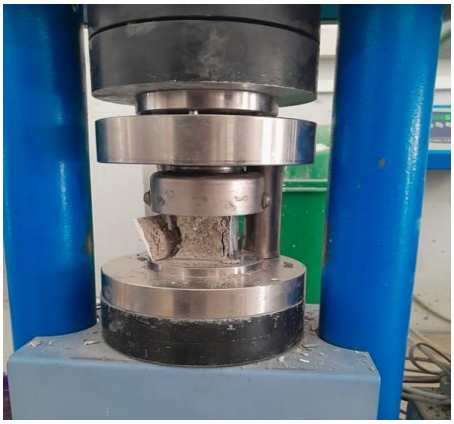

Fig. 5. Compressive strength test of geopolymer mortar

The water accessible porosity of the hardened geopolymer mortars was determined using the vacuum saturation method, following the principles outlined in NBR 9778 [49]. The specimens were first oven-dried to constant mass, then placed in a vacuum chamber and

saturated with water under vacuum conditions. The saturated surface-dry mass and the submerged mass of the specimens were then measured. The water accessible porosity was calculated as the ratio of the volume of water absorbed to the total volume of the specimen, expressed as a percentage. This test provides insights into the porosity and the ability of geopolymer mortars to absorb water, which influences their durability and transport properties. The results from these standardized tests form the basis for optimizing the geopolymer mortar formulations and understanding the effects of GP content and Ac/Pr ratio on the material's performance.

3. Results and Discussion

3.1. Analysis of Variance

The analysis of variance (ANOVA) elucidates the effects of GP content and Ac/Pr on the properties of geopolymer mortars (Table 5). For compressive strength, the ANOVA reveals that the model is statistically significant, with the intercept, Ac/Pr, GP^2, and Ac/Pr^2 all being significant factors ($p<0.05$). The linear effect of GP and the interaction term GP*Ac/Pr are not statistically significant. This suggests that the activator-to-precursor ratio has a strong influence on compressive strength, both in its linear and quadratic terms. The slump model shows significance for both GP and Ac/Pr linear effects, as well as the intercept, while the quadratic terms and interaction term are not statistically significant. For porosity, the model indicates significance for the intercept, GP^2, and Ac/Pr^2, while the linear terms and interaction are not statistically significant.

Table 5. ANOVA metrics

	Intercept	GP	Ac/Pr	GP*Ac/Pr	GP^2	Ac/Pr^2
Compressive Strength	46.7022	-0.74	2.60333	1.095	-5.04333	-4.65333
p-values	0,03	0.3376	0.0279	0.2627	0.0207	0.0257
Slump	15.5	0.916667	1.83333	-0.125	0.25	-1.57E-16
p-values	0,01	0.0154	0.0021	0.6163	0.4883	1.0000
Porosity	15.1967	-0.56	0.178333	-0.4275	1.65	3.195
p-values	0,028	0.1238	0.5473	0.2774	0.0364	0.0060

The perturbation plots (Fig. 6) offer a visual representation of these effects. For slump, both GP and Ac/Pr demonstrate positive effects, with Ac/Pr showing a stronger linear influence as indicated by its steeper slope. GP exhibits a slight curvature, suggesting a minor quadratic effect, though this is not statistically significant according to the ANOVA. The compressive strength plot reveals quadratic effects for both GP and Ac/Pr, with optimal points near the center of the design space. The Ac/Pr curve shows a more pronounced quadratic effect, consistent with its significant linear and quadratic terms in the ANOVA. The GP curve also displays a quadratic trend, but with a lower optimal point, indicating that increasing GP beyond a certain point may decrease strength. The porosity plot demonstrates strong quadratic effects for both factors, forming U-shaped curves. The Ac/Pr curve shows a more pronounced effect, especially at the extremes of the range, while the GP curve has a shallower U-shape, indicating a less severe impact on porosity at the extremes. Both factors appear to have an optimal point (minimum porosity) near the center of the design space.

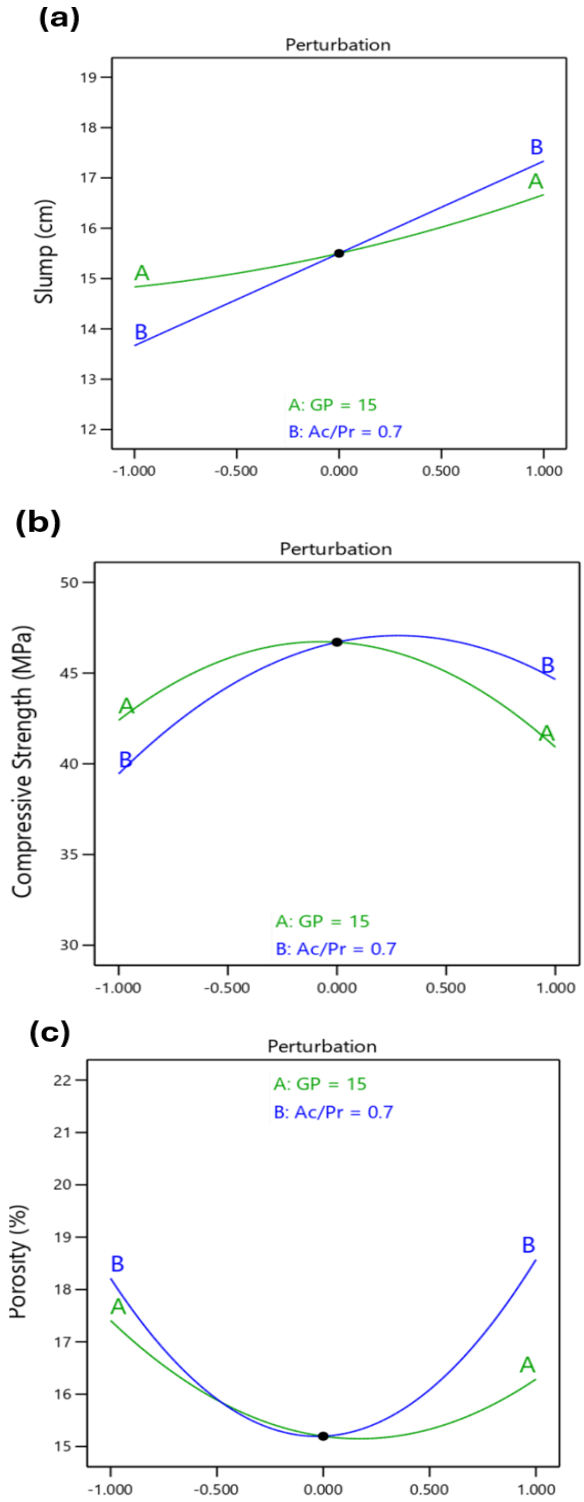

Fig. 6 Perturbation plots of (a) slump (b) compressive strength (c) porosity

These results collectively suggest that slump is positively influenced by both GP content and Ac/Pr ratio, with Ac/Pr having a stronger linear effect. Compressive strength is optimized at moderate levels of both GP and Ac/Pr, with significant quadratic effects. Porosity is minimized at moderate levels of both factors, with strong quadratic effects, particularly for Ac/Pr. These findings highlight the complex interplay between GP content and Ac/Pr ratio in determining the properties of the geopolymer mortar

3.2. Response Surface Plots

3.2.1 Slump

The contour and iso-response surface plots for the slump response (Fig. 7) provide valuable insights into the effects of GP and Ac/Pr contents on the workability of the geopolymer mortar. The contour plot, represented by the 2D color-coded image, shows a clear gradient from blue to red, indicating an increase in slump values from approximately 13 cm to 18.5 cm across the experimental range. This gradient demonstrates that both GP content and Ac/Pr ratio have significant influences on the slump of the geopolymer mortar. The iso-response curves, represented by the contour lines, further illustrate this relationship. The upward sloping nature of these curves from left to right indicates that increasing both GP content and Ac/Pr ratio generally leads to higher slump values, suggesting improved workability of the mixture. The 3D surface plot corroborates these observations, showing a rising plane from the lower left corner to the upper right corner of the plot.

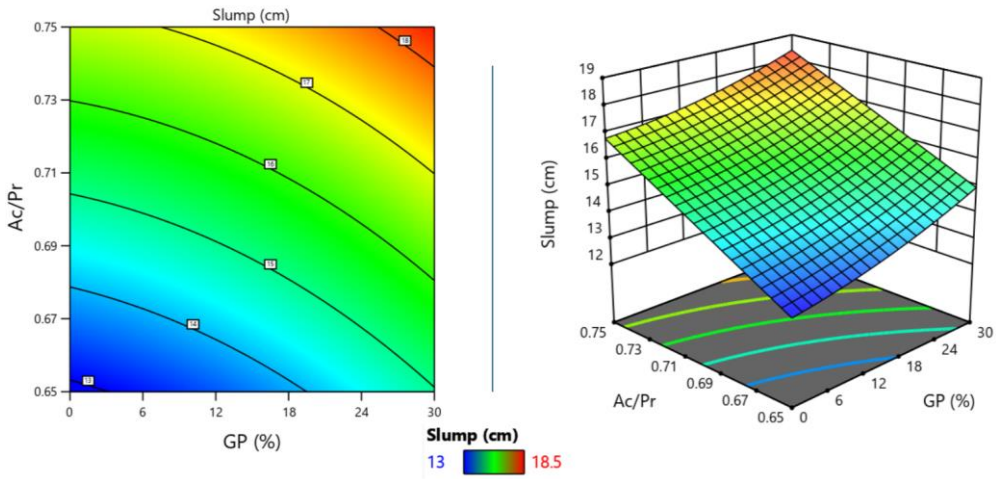

Fig. 7. Contour plot and iso-response curve of slump response

This three-dimensional representation clearly visualizes the combined effects of GP and Ac/Pr on slump. The steeper gradient along the Ac/Pr axis compared to the GP axis suggests that the Ac/Pr ratio has a more pronounced effect on slump than the GP content. This is evident from the more rapid color change and steeper slope in the Ac/Pr direction. The highest slump values, represented by the red region in the contour plot and the peak of the 3D surface, are achieved at high levels of both GP content and Ac/Pr ratio. This indicates that increasing both factors simultaneously lead to the most significant improvement in workability. Conversely, the lowest slump values, shown in blue, occur at low levels of both factors. The relatively linear nature of the iso-response curves suggests that there is limited interaction between GP and Ac/Pr in their effects on slump. Instead, they appear to have additive effects, with each factor independently contributing to increased workability. This linear trend aligns with the earlier ANOVA results, which

showed significant linear effects for both factors on slump. The continuous increase in slump with increasing GP content can be attributed to the spherical nature of GP particles, which may enhance the flowability of the mixture [30]. The positive effect of increasing Ac/Pr ratio on slump is likely due to the higher liquid content in the mixture, which naturally improves workability.

3.2.2 Compressive Strength

The contour and iso-response surface plots for compressive strength (Fig. 8) reveal a complex relationship between GP and Ac/Pr, and the mechanical performance of the geopolymer mortar. The plots exhibit a distinct dome-shaped surface, indicating the presence of an optimal region for compressive strength. This optimal zone is centered around 14.2% GP content and 0.71 Ac/Pr ratio, where the highest compressive strength values are achieved. The contour plot shows concentric elliptical patterns, with the peak strength region colored in red at the center. As we move away from this optimal point, the colors transition through yellow and green to blue, representing a gradual decrease in compressive strength. This pattern suggests that both excess and insufficient amounts of GP or Ac/Pr can lead to reduced strength performance.

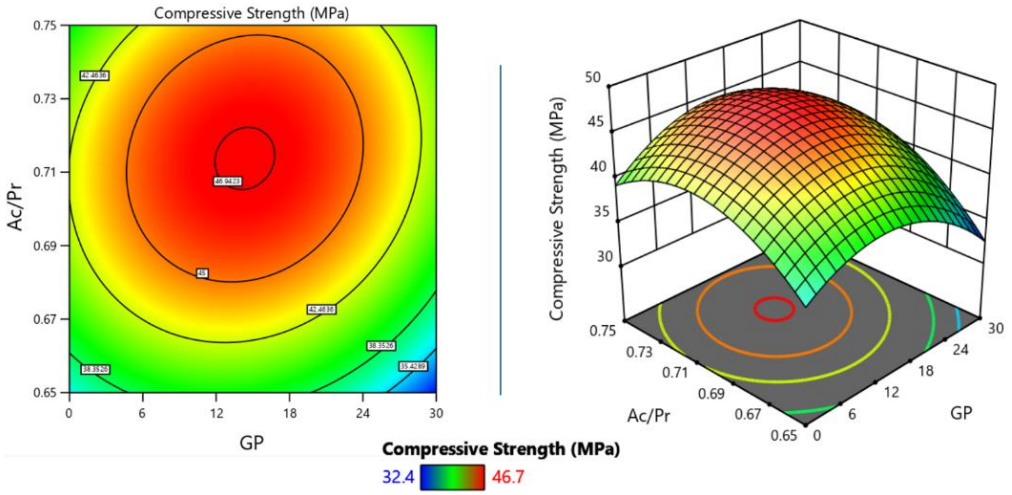

Fig. 8. Contour plot and iso-response curve of compressive strength response

The 3D surface plot further emphasizes this quadratic relationship, displaying a clear peak in the central region. The curvature of the surface is more pronounced along the Ac/Pr axis compared to the GP axis, indicating that the Ac/Pr ratio has a more significant impact on compressive strength than GP content. This observation aligns with the ANOVA results, which showed that both linear and quadratic terms for Ac/Pr were statistically significant.

The existence of an optimal region can be explained by considering the effects of GP and Ac/Pr on the geopolymerization process and the resulting microstructure. The incorporation of GP introduces additional silica into the system, which can modify the Ca/Si and Si/Al ratios of the binder phase. At the optimal GP content (around 14%), there is likely an ideal balance between these ratios that promotes the formation of a strong and stable calcium aluminosilicate hydrate (C-A-S-H) gel structure.

The C-A-S-H gel, which is the primary binding phase in slag-based geopolymers, is sensitive to the Ca/Si ratio. As GP content increases, it initially enhances the Si/Al ratio, potentially leading to a more polymerized and stronger gel structure [24]. However, beyond the optimal point, excessive silica may disrupt the balance, possibly leading to unreacted

particles or a weaker gel structure, thus explaining the decrease in strength at higher GP levels.

The Ac/Pr ratio plays a crucial role in providing the alkaline environment necessary for the dissolution of slag and GP particles and subsequent geopolymerization. The optimal Ac/Pr ratio of 0.71 likely represents the point where there is sufficient alkaline activator to promote adequate dissolution and reaction of the precursors, without excess liquid that could lead to increased porosity and reduced strength.

The significant quadratic effects observed in the ANOVA for both GP^2 and Ac/Pr^2 support the curvilinear relationship seen in the response surface plots. These quadratic effects indicate that both factors have an optimal range, beyond which their benefits diminish or become detrimental to strength development. The interaction between GP content and Ac/Pr ratio, while not statistically significant according to the ANOVA, may still play a subtle role in determining the exact shape and position of the optimal region. This interaction could be related to how the alkaline activator interacts with the different proportions of slag and GP, affecting the dissolution rates and the formation of reaction products.

3.2.3 Porosity

The contour plot and iso-response surface plot for porosity (Fig. 9) reveal a complex relationship between GP content, Ac/Pr ratio, and the resulting porosity of slag-based geopolymer mortars. The optimal region for minimizing porosity is observed corresponding to 17% GP and 0.7 Ac/Pr ratio, where porosity values reach their minimum of around 15%. As we move away from this optimal region, porosity increases, reaching a maximum of about 21.5% at high GP content and high Ac/Pr ratio.

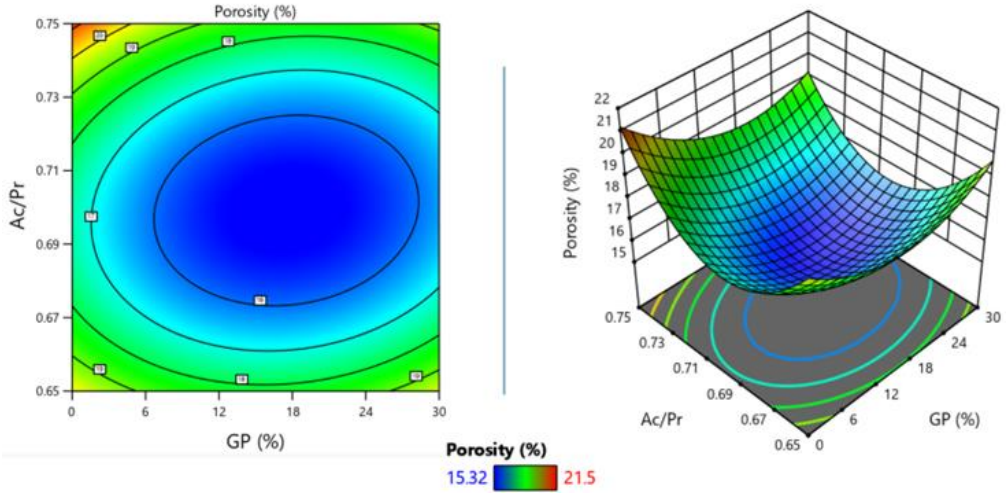

Fig. 9. Contour plot and iso-response curve of porosity response

The interaction between GP content and Ac/Pr ratio is evident from the non-linear contour lines and curved surface in the 3D plot. This interaction suggests that the impact of GP on porosity is influenced by the Ac/Pr ratio, and vice versa. At lower Ac/Pr ratios, the effect of increasing GP content on porosity is less pronounced, possibly because there is insufficient activator to fully react with the glass powder, leading to a more compact structure with unreacted GP particles filling voids. Conversely, at higher Ac/Pr ratios, increasing GP content has a more significant effect on porosity, as there is more liquid available to react with the GP, potentially creating a more open pore structure.

The optimal region of low GP content and low Ac/Pr ratio likely represents a balance where there is sufficient activator to react with the slag precursor without excess liquid, resulting in a denser C-A-S-H gel network with lower porosity. In this region, the formation of C-A-S-H gel is maximized, and the development of voids is minimized. As we move away from this optimal region, either by increasing GP content or Ac/Pr ratio, the balance is disrupted, leading to increased porosity through different mechanisms. Higher GP content may result in more unreacted particles and a less interconnected C-A-S-H gel network, while higher Ac/Pr ratios may lead to excess liquid that creates additional voids upon evaporation, thus increasing the absorption capacity of mortars. This phenomenon can be attributed to the formation of capillary pores as the liquid phase evaporates, leaving behind voids that contribute to a more porous microstructure. The study by Das et al. [50]emphasizes that elevated water absorption values are typically correlated with increased surface porosity. This surface porosity not only influences the immediate physical and mechanical properties of the mortar but also has long-term implications on its durability.

At higher Ac/Pr ratios, the increase in porosity is accompanied by a decrease in compressive strength. This inverse relationship can be explained by the fact that the presence of more voids within the mortar matrix reduces the density and integrity of the structure, leading to weaker mechanical performance. As the porosity increases, the material's ability to bear loads diminishes, which directly affects its compressive strength. Moreover, the interconnected pore network created by the excess liquid not only weakens the material but also makes it more susceptible to the ingress of harmful agents, further compromising its structural capacity over time.

3.3. Model Diagnostics

To create thorough regression models for a range of response variables, the central composite design was used. Strong predictive performance is shown in the fit summary for these models (Table 6), where high R-squared values, ranging from 0.96 to 0.98, indicate excellent model fit. The models are assessed using the mean response values as baseline standards. Furthermore, for all replies, the appropriate precision values—which evaluate the signal-to-noise ratio—are significantly higher than the suggested cutoff point of 4. This suggests that the models have a strong capacity to consistently navigate the design space, indicating that they are appropriate for forecasting how GP and Ac/Pr would affect the properties of mortar.

Table 6. Fit summary

Response	Mean	R^2	Adjusted R^2	Adeq. Precision
Slump (cm)	15.67	0.98	0.93	15.01
Compressive strength (MPa)	40.24	0.95	0.86	10.87
Porosity (%)	18.43	0.96	0.89	11.4

The model's accurate predictions across the range of each response variable are shown in the actual vs predicted plots (Fig. 10). The model's predictions and the actual data are well aligned in these graphs, demonstrating the validity and dependability of the regression models created with the central composite design. This alignment is further supported by the strong R-squared values, which demonstrate the models' capacity to represent the underlying relationships between the response variables and the input factors.

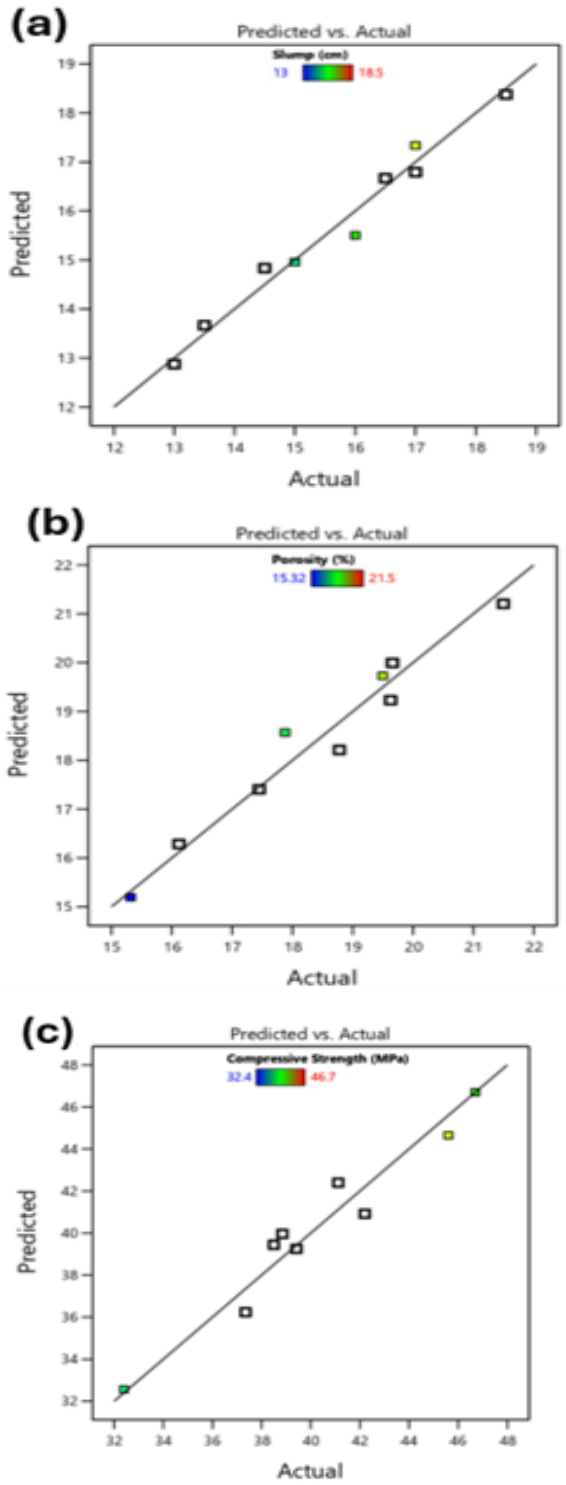

Fig. 10. Actual by predicted plots of (a) slump (b) compressive strength (c) porosity

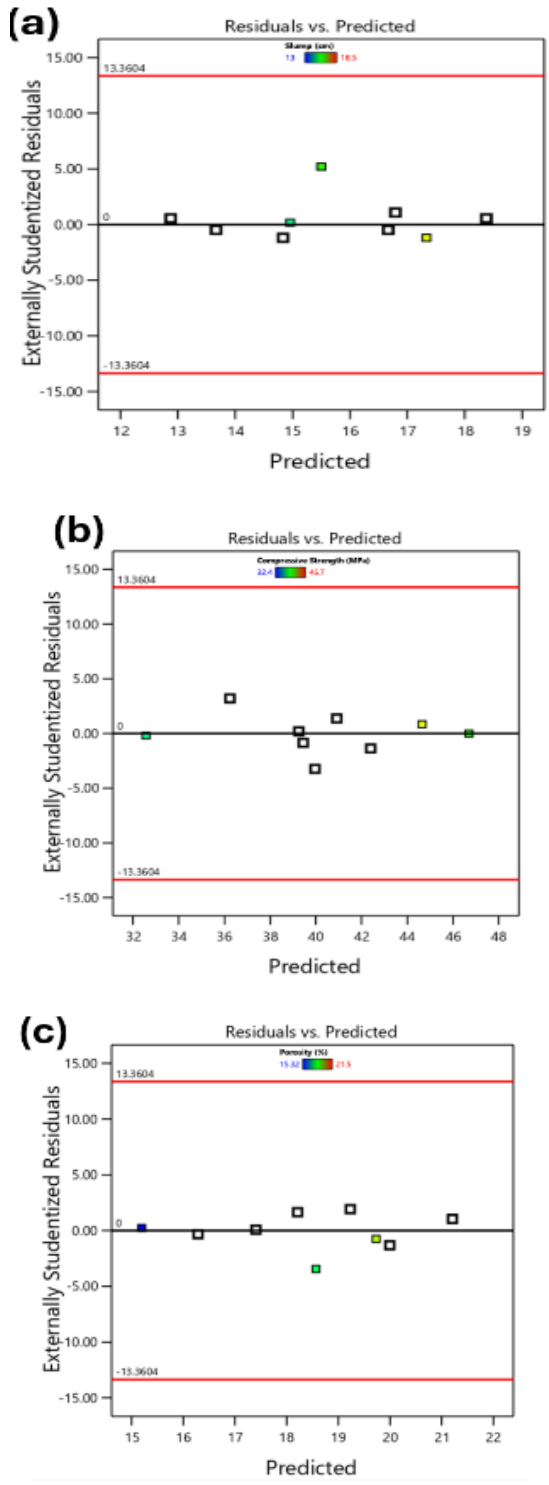

Fig. 11. Residual vs predicted plots of (a) slump (b) compressive strength (c) porosity

Furthermore, the residual plots (Fig. 11) show a random residual dispersion around zero, suggesting that the models have successfully and fairly accounted for the data's variability. This randomness shows that all systematic patterns have been described by the regression models and that the models are well-specified. This demonstrates how well the models capture the important correlations between the response and input variables. The central composite design was used to create all-encompassing regression equations for porosity, compressive strength, and slump. The complex relationship between GP content and Ac/Pr ratio is described by the slump equation Eq. (1), a model of second-order polynomials. The link between Ac/Pr and GP, which includes their interaction, is revealed by the compressive strength model (Eq. (2)). The impact of Ac/Pr and GP on porosity is illustrated by the porosity equation, Eq. (3).

$$Slump\ (cm) = 15.5 + 0.92 * GP + 1.83 * Ac/Pr - 0.125 * GP * Ac/Pr + 0.25 * GP^2 - 1.57e\text{^}(-16) * Ac/Pr^2 \quad (1)$$

$$Compressive\ strength\ (MPa) = 46.7 - 0.74 * GP + 2.6 * Ac/Pr + 1.09 * GP * Ac/Pr - 5.04 * GP^2 - 4.65 * Ac/Pr^2 \quad (2)$$

$$Porosity\ (\%) = 15.1967 - 0.56 * GP + 0.178333 * Ac/Pr - 0.4275 * GP * Ac/Pr + 1.65 * GP^2 + 3.195 * Ac/Pr^2 \quad (3)$$

3.4. SEM/EDX Analysis

Microstructural analysis was conducted using SEM to investigate the morphological characteristics and compositional nature of the geopolymer matrices. Fig. 12 presents SEM micrographs of two key specimens: M1 (0% GP and 0.65 Ac/Pr) and M5 (15% GP and 0.7 Ac/Pr). The SEM image of specimen M1 reveals a heterogeneous microstructure characterized by the presence of C-A-S-H gels, which appear as the predominant binding phase. These C-A-S-H formations are evident as dense, amorphous regions within the matrix. The microstructure also exhibits notable features such as pores and microcracks. The presence of pores, varying in size and distribution, indicates the complex nature of the geopolymerization process and its impact on the material's porosity. In contrast, the SEM micrograph of specimen M5 demonstrates a more refined and homogeneous microstructure. The incorporation of 15% GP and the slightly higher Ac/Pr ratio (0.7) appear to have resulted in a denser matrix with fewer visible pores and cracks. The C-A-S-H gel formation in M5 seems more uniform and interconnected, suggesting a more complete geopolymerization reaction. This observation is consistent with the work of Zhang et al. [51] who found that the incorporation of GP in slag based-geopolymers leads to a more compact microstructure.

To confirm the chemical composition of the binding phases, EDX spectroscopy was performed on three distinct points within the samples, as indicated in Fig. 13. The EDX spectra reveal the elemental composition of the C-A-S-H gels, which are primarily composed of O, Si, Al, Na, and Ca, with minor amounts of Mg. Spectrum (1) shows a high content of Si (21.05%) and O (38.98%), indicative of the silica-rich nature of the geopolymer gel. The presence of Al (5.81%) and Na (11.53%) confirms the formation of sodium aluminosilicate hydrate (N-A-S-H) gels, which are typical in geopolymer systems. The notable Ca content (9.99%) suggests the coexistence of C-A-S-H gels, likely due to the calcium-rich nature of the slag precursor. These findings are in line with recent research by Wang et al. [52], who observed similar elemental distributions in slag-based geopolymers and highlighted the importance of Ca in forming robust C-A-S-H networks. Spectra (2) and (3) show similar elemental compositions but with varying proportions. The increase in Ca content from spectrum (1) to (2) (14.23%) and (3) (21.23%) indicates a higher degree of C-A-S-H gel formation in these regions. This variation in Ca content

across different points suggests a heterogeneous distribution of reaction products within the geopolymer matrix.

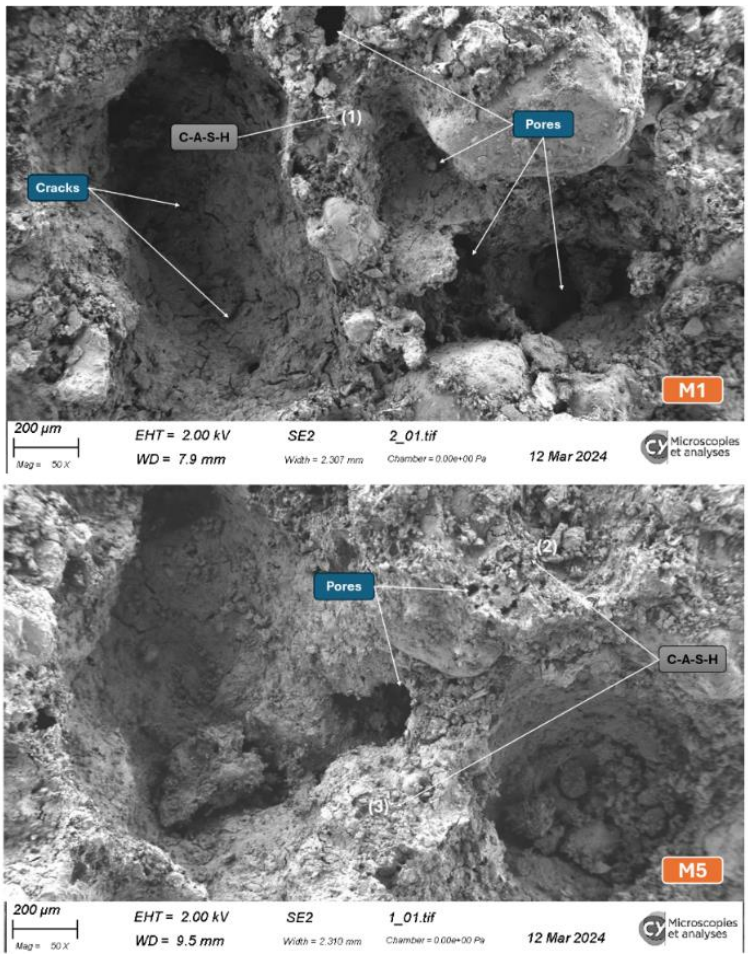

Fig. 12. Scanning electron microscopy micrographs of key mixtures M1 and M5

The presence of Mg in all spectra (1.63%, 0.77%, and 3.06% respectively) can be attributed to the MgO content in the original slag, which has been incorporated into the gel structure during geopolymerization, a phenomenon also reported by Chitsaz et al. [53] and Jin et al. [54] in their study of alkali-activated slag systems. The EDX results corroborate the visual observations from the SEM images, confirming the formation of C-A-S-H gels as the primary binding phase in these slag-based geopolymers. The incorporation of GP in specimen M5 appears to have promoted a more uniform distribution of these gels, resulting in a denser and potentially more durable microstructure. This is consistent with findings by Varma et al. [55] , who demonstrated that the addition of GP in geopolymers leads to a more homogeneous gel formation due to the pore-filling effect of fine glass particles and enhanced dissolution of silica.

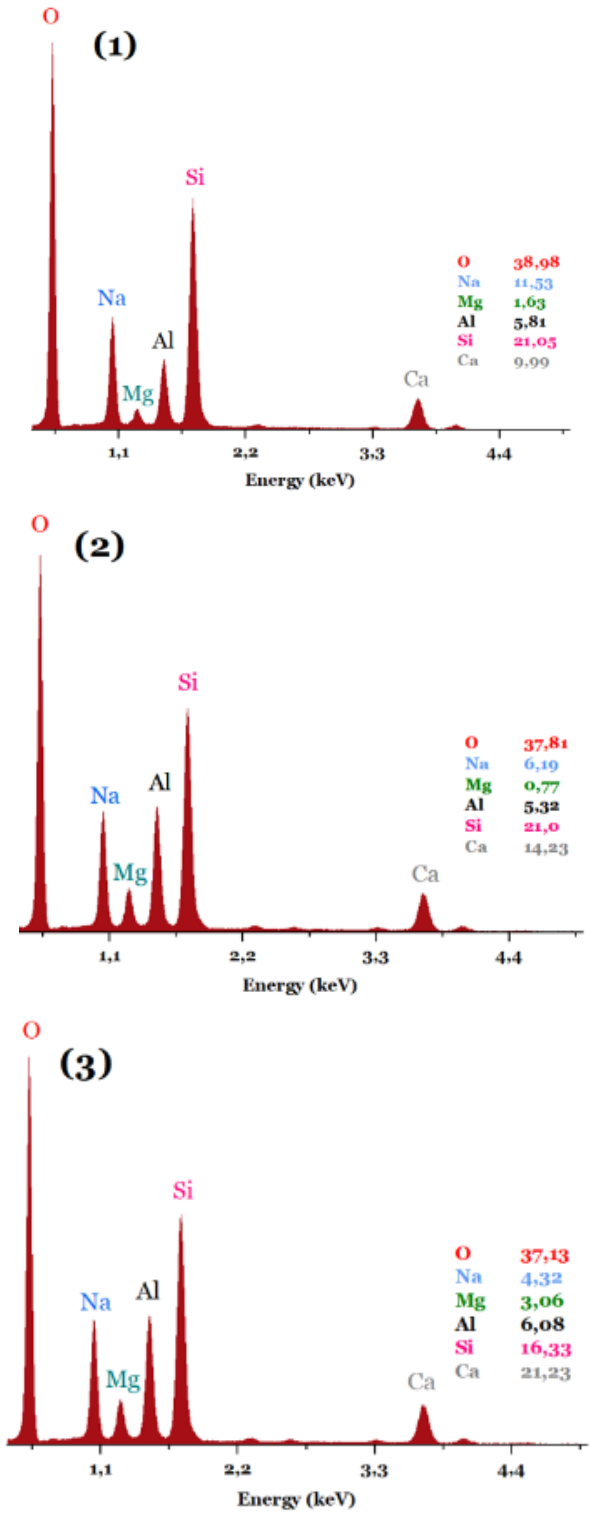

Fig. 13. EDX spectra of identified points in key mixtures M1 and M5

3.5. Optimization

Using a desirable approach, the formulation of the geopolymer mortar was fine-tuned to achieve maximum slump and compressive strength with minimum porosity. Considering their weights and relative importance, the desirability method enables the optimization of numerous responses at once (Table 7). Level 5 weight 0.5 was given to compressive strength because of its crucial significance in determining the geopolymer system's long-term structural performance. Since the slump is so important for making sure the mortar is workable, it was given a weight of 0.3 and an importance level of 5. As a measure of durability that does not have an immediate effect, porosity was given the lowest weight of 0.2 and the fifth most important level.

Table 7. Criteria of desirability analysis

Name	Goal	Lower Limit	Upper Limit	Lower Weight	Upper Weight	Importance
Compressive Strength (MPa)	maximize	32.4	46.7	0.5	1	5
Slump (cm)	maximize	13	18.5	0.3	1	5
Porosity (%)	minimize	15.32	21.5	1	0.2	5

The optimal formulation that comes from the desirability analysis may be easily seen in Fig. 14's contour and iso-response plots. A GP content of 18.2% and an Act/Pr ratio of 0.72 are recommended by the ideal solution.

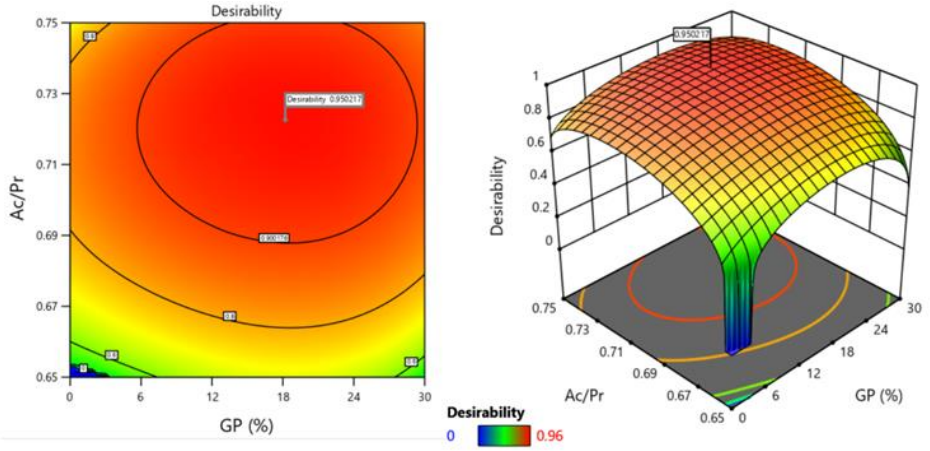

Fig. 14. Contour plot and iso-response curve of optimized formulation

For this optimized mixture, the predicted outcomes are shown in Fig. 15: a slump of 16.53 cm, a compressive strength of 46.64 MPa, and a porosity of 15.85%. A high level of satisfaction with the goals and importance levels assigned to each answer variable is shown by the total desirability value obtained of 0.95.

The point prediction (Table 8) provides valuable statistical information about the predicted responses for the optimized formulation of the slag-based geopolymer mortar. The predicted mean compressive strength of 46.64 MPa, slump of 16.52 cm, and porosity of 15.85% all demonstrate favorable performance characteristics. The relatively small standard deviations for each property (1.59204 MPa, 0.448764 cm, and 0.645938% respectively) indicate good consistency in the mix. The narrow 95% confidence intervals for all three properties suggest high precision in the predictions. The wider 95% tolerance intervals for 99% of the population account for natural variability between samples, with

compressive strength ranging from 32.14 to 61.14 MPa, slump from 12.44 to 20.61 cm, and porosity from 9.96% to 21.73%.

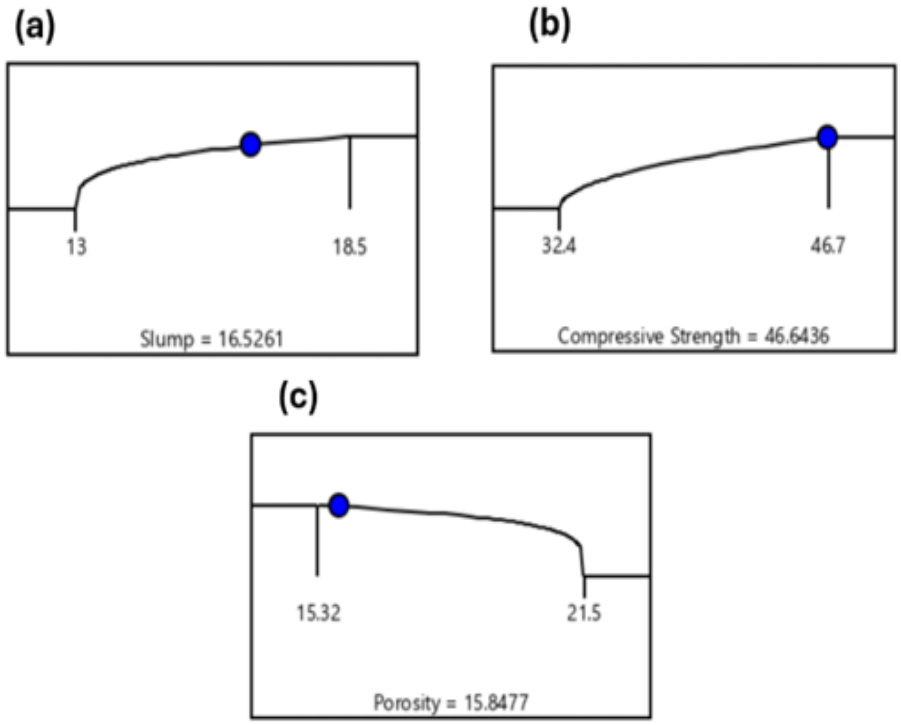

Fig. 15. Predicted responses of (a) slump (b) compressive strength (c) porosity

The relatively narrow confidence intervals for all responses indicate good precision in the predictions, suggesting the model is well-fitted to the experimental data. The small standard deviations, particularly for slump and porosity, suggest that the optimized formulation should produce consistent results in terms of workability and microstructure. The predicted compressive strength is robust, with even the lower bound of the tolerance interval (32.14 MPa) being acceptable for many applications. This indicates that the optimized mix is likely to meet strength requirements consistently.

Table 8. Point prediction

Response	Compressive Strength (MPa)	Slump (cm)	Porosity (%)
Predicted Mean	46.6436	16.5261	15.8477
Predicted Median	46.6436	16.5261	15.8477
Std Dev	1.59204	0.448764	0.645938
SE Mean	1.07329	0.302541	0.435469
95% CI low for Mean	43.2279	15.5633	14.4619
95% CI high for Mean	50.0593	17.4889	17.2336
95% TI low for 99% Pop	32.1433	12.4387	9.96452
95% TI high for 99% Pop	61.1439	20.6134	21.7309

The predicted slump range suggests good workability, with even the extremes of the tolerance interval (12.44 to 20.61 cm) being manageable for most construction applications. While the mean porosity prediction is good, the wider tolerance interval reflects the inherent variability in this property. This variability should be considered when designing for applications where porosity is critical. The fact that all responses have reasonably narrow prediction ranges suggests that the optimized formulation is robust and should perform consistently across batches.

4. Conclusions

This comprehensive investigation into the impact of GP incorporation and Ac/Pr ratio on slag-based geopolymer mortars has produced several key insights:

- The use of central composite design and response surface methodology proved effective in modeling and optimizing the complex interactions between input factors (GP content and Ac/Pr ratio) and response variables (slump, compressive strength, and porosity). These approaches provided reliable predictive models for each response variable, evidenced by high R-squared values (ranging from 0.95 to 0.98) and narrow confidence intervals, laying a strong foundation for future geopolymer optimization studies.
- GP content and Ac/Pr ratio were found to significantly influence the properties of slag-based geopolymer mortars, with their effects varying across different performance metrics. This emphasizes the necessity of precisely controlling these variables to achieve targeted performance outcomes.
- Workability, as measured by slump, generally improved with increased GP content and Ac/Pr ratio, likely due to the spherical nature of glass particles and the higher content of activators. This has practical implications for improving the placement and compaction of geopolymer mortars in construction settings.
- Compressive strength displayed a quadratic relationship with both factors, reaching its peak at moderate GP content and Ac/Pr ratios, indicating an optimal formation of C-A-S-H gel structures. The highest compressive strength was achieved with 14.2% GP and a 0.71 Ac/Pr ratio, demonstrating that these optimized mixes can meet or exceed the strength requirements of many construction applications.
- Porosity was minimized at moderate levels of both factors, with notable quadratic effects, especially for the Ac/Pr ratio. This underlines the need for a carefully balanced mix design to achieve a dense microstructure while preserving sufficient workability.
- Microstructural analysis using SEM and EDX revealed that incorporating GP at optimal levels (e.g., specimen M5 with 15% GP) led to a more refined and homogenous microstructure with a denser C-A-S-H gel network. The EDX spectra confirmed that C-A-S-H gels were the primary binding phase, with elemental composition varying across different matrix regions. This microstructural improvement supports the observed gains in mechanical properties and reduced porosity at optimal GP content and Ac/Pr ratios.
- Desirability analysis identified an optimal formulation with 18.2% GP content and a 0.72 Ac/Pr ratio, balancing workability, strength, and porosity. The optimized mixture is predicted to yield a slump of 16.53 cm, a compressive strength of 46.64 MPa, and a porosity of 15.85%, making it well-suited for practical applications.
- The predictive models developed in this study demonstrated high accuracy and robustness, as reflected in the strong R-squared values and narrow confidence intervals.

These findings highlight the potential for using GP in slag-based geopolymer systems, contributing to more sustainable construction materials without compromising performance. The optimization approach presented offers a valuable methodology for customizing geopolymer mix designs to meet specific performance goals.

Future research should focus on long-term durability assessments of these optimized mixtures, as well as evaluating their performance under varying curing conditions and environmental exposures. Additionally, life cycle assessments could further quantify the environmental advantages of incorporating waste glass in geopolymer formulations.

Acknowledgement

The authors would like to extend their gratitude to the Civil Engineering Laboratory at the University of Bordj Bou Arreridj for their assistance in facilitating the experimental work for this study.

References

[1] Benhelal E, Zahedi G, Shamsaei Ezzatollah A, Bahadori B. Global strategies and potentials to curb CO2 emissions in cement industry. J Clean Prod. 2013 Jul;51:142-61. https://doi.org/10.1016/j.jclepro.2012.10.049
[2] Sandanayake M, Gunasekara C, Law D, Zhang G, Setunge S. Greenhouse gas emissions of different fly ash based geopolymer concretes in building construction. J Clean Prod. 2018;204:399-408. https://doi.org/10.1016/j.jclepro.2018.08.311
[3] McLellan BC, Williams RP, Lay J, Van Riessen A, Corder GD. Costs and carbon emissions for geopolymer pastes in comparison to ordinary portland cement. J Clean Prod. 2011 Jun;19(9-10):1080-90. https://doi.org/10.1016/j.jclepro.2011.02.010
[4] Davidovits J. Geopolymers and geopolymeric materials. J Therm Anal. 1989;35(2):429-41. https://doi.org/10.1007/BF01904446
[5] Krishna RS, et al. A review on developments of environmentally friendly geopolymer technology. Materialia (Oxf). 2021;20:101212. https://doi.org/10.1016/j.mtla.2021.101212
[6] Ren B, Zhao Y, Bai H, Kang S, Zhang T, Song S. Eco-friendly geopolymer prepared from solid wastes: A critical review. Chemosphere. 2021;267:128900. https://doi.org/10.1016/j.chemosphere.2020.128900
[7] Odeh A, et al. Recent progress in geopolymer concrete technology: A review. Iranian J Sci Technol Trans Civ Eng. 2024. https://doi.org/10.1007/s40996-024-01391-z
[8] Xu H, Van Deventer JSJ. The geopolymerisation of alumino-silicate minerals. Int J Miner Process. 2000;59(3):247-66. https://doi.org/10.1016/S0301-7516(99)00074-5
[9] Van Jaarsveld JGS, Van Deventer JSJ, Lorenzen L. Factors affecting the immobilization of metals in geopolymerized flyash. Metall Mater Trans B. 1998;29(1):283-91. https://doi.org/10.1007/s11663-998-0032-z
[10] Das D, Rout PK. A review of coal fly ash utilization to save the environment. Water Air Soil Pollut. 2023;234(2):128. https://doi.org/10.1007/s11270-023-06143-9
[11] Matsimbe J, Dinka M, Olukanni D, Musonda I. Geopolymer: A systematic review of methodologies. Materials. 2022;15(19. https://doi.org/10.3390/ma15196852
[12] Biernacki JJ, et al. Cements in the 21st century: challenges, perspectives, and opportunities. J Am Ceram Soc. 2017;100(7):2746-73. https://doi.org/10.1111/jace.14948
[13] Davidovits J. Geopolymer cement. A review. Geopolymer Institute, Technical papers. 2013;21:1-11. https://doi.org/10.1520/STP156620120106
[14] Kozhukhova N, Kozhukhova M, Teslya A, Nikulin I. The effect of different modifying methods on physical, mechanical and thermal performance of cellular geopolymers as

thermal insulation materials for building structures. Buildings. 2022 Feb;12(2). https://doi.org/10.3390/buildings12020241
[15] Dabbebi R, Barroso de Aguiar JL, Camões A, Samet B, Baklouti S. Effect of the calcinations temperatures of phosphate washing waste on the structural and mechanical properties of geopolymeric mortar. Constr Build Mater. 2018;185:489-98. https://doi.org/10.1016/j.conbuildmat.2018.07.045
[16] Gadkar A, Subramaniam KVL. Tailoring porosity and pore structure of cellular geopolymers for strength and thermal conductivity. Constr Build Mater. 2023;393:132150. https://doi.org/10.1016/j.conbuildmat.2023.132150
[17] Huseien GF, Mirza J, Ismail M, Hussin MW. Influence of different curing temperatures and alkali activators on properties of GBFS geopolymer mortars containing fly ash and palm-oil fuel ash. Constr Build Mater. 2016;125:1229-40. https://doi.org/10.1016/j.conbuildmat.2016.08.153
[18] Puligilla S, Mondal P. Role of slag in microstructural development and hardening of fly ash-slag geopolymer. Cem Concr Res. 2013;43:70-80. https://doi.org/10.1016/j.cemconres.2012.10.004
[19] Fu C, Ye H, Zhu K, Fang D, Zhou J. Alkali cation effects on chloride binding of alkali-activated fly ash and metakaolin geopolymers. Cem Concr Compos. 2020;114:103721. https://doi.org/10.1016/j.cemconcomp.2020.103721
[20] Berkouche A, et al. Enhancing sustainable construction practices: Utilizing heat-treated recycled concrete fines for improving slag-based geopolymer materials. Arab J Sci Eng. 2024. https://doi.org/10.1007/s13369-024-09477-6
[21] Swathi B, Vidjeapriya R. Influence of precursor materials and molar ratios on normal, high, and ultra-high performance geopolymer concrete-A state of art review. Constr Build Mater. 2023;392:132006. https://doi.org/10.1016/j.conbuildmat.2023.132006
[22] Komnitsas K, Zaharaki D. Utilisation of low-calcium slags to improve the strength and durability of geopolymers. 2009; 343-375. https://doi.org/10.1533/9781845696382.2.343
[23] Wu X, Shen Y, Hu L. Performance of geopolymer concrete activated by sodium silicate and silica fume activator. Case Studies in Construction Materials. 2022 Dec;17:e01513. https://doi.org/10.1016/j.cscm.2022.e01513
[24] Kim G, et al. Evaluation of the thermal stability of metakaolin-based geopolymers according to Si/Al ratio and sodium activator. Cem Concr Compos. 2024;150:105562. https://doi.org/10.1016/j.cemconcomp.2024.105562
[25] Duxson P, Provis JL. Designing precursors for geopolymer cements. J Am Ceram Soc. 2008;91(12):3864-9. https://doi.org/10.1111/j.1551-2916.2008.02787.x
[26] Bernal SA, et al. Gel nanostructure in alkali-activated binders based on slag and fly ash, and effects of accelerated carbonation. Cem Concr Res. 2013;53:127-44. https://doi.org/10.1016/j.cemconres.2013.06.007
[27] Wang R, Zhou X, Zhang W, Ye J, Wang J. Transport mechanism of uranyl nitrate in nanopore of geopolymer with different Si/Al ratios: Molecular dynamics simulation. J Solid State Chem. 2024;331:124542. https://doi.org/10.1016/j.jssc.2023.124542
[28] Varma DN, Singh SP. A review on waste glass-based geopolymer composites as a sustainable binder. Silicon. 2023;15(18):7685-703. https://doi.org/10.1007/s12633-023-02629-7
[29] Mendes BC, et al. Evaluation of eco-efficient geopolymer using chamotte and waste glass-based alkaline solutions. Case Stud Constr Mater. 2022;16. https://doi.org/10.1016/j.cscm.2021.e00847
[30] Belkadi AA, et al. Experimental investigation into the potential of recycled concrete and waste glass powders for improving the sustainability and performance of cement mortars properties. Sustain Energy Technol Assess. 2024;64:103710. https://doi.org/10.1016/j.seta.2024.103710

[31] Xiao R, et al. Strength, microstructure, efflorescence behavior and environmental impacts of waste glass geopolymers cured at ambient temperature. J Clean Prod. 2020;252:119610. https://doi.org/10.1016/j.jclepro.2019.119610
[32] Varma DN, Singh SP. Recycled waste glass as precursor for synthesis of slag-based geopolymer. Mater Today Proc. 2023.
[33] Singh RJ, Raut A, Murmu AL, Jameel M. Influence of glass powder incorporated foamed geopolymer blocks on thermal and energy analysis of building envelope. J Build Eng. 2021;43:102520. https://doi.org/10.1016/j.jobe.2021.102520
[34] Khan MNN, Kuri JC, Sarker PK. Effect of waste glass powder as a partial precursor in ambient cured alkali activated fly ash and fly ash-GGBFS mortars. J Build Eng. 2021;34:101934. https://doi.org/10.1016/j.jobe.2020.101934
[35] Hosseini S, Brake NA, Nikookar M, Günaydın-Şen Ö, Snyder HA. Mechanochemically activated bottom ash-fly ash geopolymer. Cem Concr Compos. 2021;118:103976. https://doi.org/10.1016/j.cemconcomp.2021.103976
[36] Zheng K. Pozzolanic reaction of glass powder and its role in controlling alkali-silica reaction. Cem Concr Compos. 2016;67:30-8. https://doi.org/10.1016/j.cemconcomp.2015.12.008
[37] Zhang B, He P, Poon CS. Optimizing the use of recycled glass materials in alkali activated cement (AAC) based mortars. J Clean Prod. 2020;255:120228. https://doi.org/10.1016/j.jclepro.2020.120228
[38] Dey A, et al. Towards net-zero emission: A case study investigating geopolymer concrete's sustainability potential using recycled glass powder and gold mine tailings. J Build Eng. 2024;108683. https://doi.org/10.1016/j.jobe.2024.108683
[39] Siddika A, Hajimohammadi A, Ferdous W, Sahajwalla V. Roles of waste glass and the effect of process parameters on the properties of sustainable cement and geopolymer concrete-A state-of-the-art review. Polymers (Basel). 2021;13(22). https://doi.org/10.3390/polym13223935
[40] Nath SK, Kumar S. Role of particle fineness on engineering properties and microstructure of fly ash derived geopolymer. Constr Build Mater. 2020 Feb;233:117294. https://doi.org/10.1016/j.conbuildmat.2019.117294
[41] Das D, Rout PK. Synthesis and characterization of fly ash and gbfs based geopolymer material. Biointerface Res Appl Chem. 2021;11(6):14506-19. https://doi.org/10.33263/BRIAC116.1450614519
[42] Das D, Rout PK. Synthesis, characterization and properties of fly ash based geopolymer materials. J Mater Eng Perform. 2021;30(5):3213-31. https://doi.org/10.1007/s11665-021-05647-x
[43] Kumar S, Mucsi G, Kristály F, Pekker P. Mechanical activation of fly ash and its influence on micro and nano-structural behaviour of resulting geopolymers. Adv Powder Technol. 2017 Mar;28(3):805-13. https://doi.org/10.1016/j.apt.2016.11.027
[44] Debnath K, Das D, Rout PK. Effect of mechanical milling of fly ash powder on compressive strength of geopolymer. Mater Today Proc. 2022 Jan;68:242-9. https://doi.org/10.1016/j.matpr.2022.08.321
[45] Yadav M, et al. Optimizing the fly ash/activator ratio for a fly ash-based geopolymer through a study of microstructure, thermal stability, and electrical properties. Ceramics. 2023;6(4):2352-66. https://doi.org/10.3390/ceramics6040144
[46] Nana A, et al. Mechanical performance, phase evolution and microstructure of natural feldspathic solid solutions consolidated via alkali activation: Effect of NaOH concentration. Silicon. 2022;14(8):4107-20. https://doi.org/10.1007/s12633-021-01193-2
[47] ASTM C. Standard test method for slump of hydraulic-cement concrete. ASTM International West Conshohocken, PA; 2012.
[48] EN-196-1. Methods of testing cement-Part 1: Determination of strength. Quality and Standards Authority of Ethiopia, ES; 2005.

[49] Técnicas ABDN. NBR 9778: Argamassa e concreto endurecidos-Determinação da absorção de água, índices de vazios e massa específica. Rio de Janeiro; 2005.
[50] Das D, Rout PK. Synthesis of inorganic polymeric materials from industrial solid waste. Silicon. 2023;15(4):1771-91. https://doi.org/10.1007/s12633-022-02116-5
[51] Zhang L, Yue Y. Influence of waste glass powder usage on the properties of alkali-activated slag mortars based on response surface methodology. Constr Build Mater. 2018 Aug;181:527-34. https://doi.org/10.1016/j.conbuildmat.2018.06.040
[52] Wang J, Wu D, Chen K, Mao N, Zhang Z. Effect of Ca content on the synthesis and properties of FA-GGBFS geopolymer: Combining experiments and molecular dynamics simulation. J Build Eng. 2024 Oct;94:109908. https://doi.org/10.1016/j.jobe.2024.109908
[53] Chitsaz S, Tarighat A. Estimation of the modulus of elasticity of N-A-S-H and slag-based geopolymer structures containing calcium and magnesium ions as impurities using molecular dynamics simulations. Ceram Int. 2021 Mar;47(5):6424-33. https://doi.org/10.1016/j.ceramint.2020.10.224
[54] Jin F, Gu K, Al-Tabbaa A. Strength and hydration properties of reactive MgO-activated ground granulated blastfurnace slag paste. Cem Concr Compos. 2015 Mar;57:8-16. https://doi.org/10.1016/j.cemconcomp.2014.10.007
[55] Varma DN, Singh SP. Recycled waste glass as precursor for synthesis of slag-based geopolymer. Mater Today Proc. 2023 Mar.